

HIGH FREQUENCY MICROMECHANICAL PIEZO-ON-SILICON BLOCK RESONATORS

Shweta Humad, Reza Abdolvand, Gavin K. Ho, Gianluca Piazza and Farrokh Ayazi

School of Electrical and Computer Engineering
Georgia Institute of Technology
Atlanta, Georgia 30332-0250 USA

shweta@ece.gatech.edu; ayazi@ece.gatech.edu; Tel: (404) 894-9496; Fax: (404) 894-4700

ABSTRACT

This paper reports on the design, implementation and characterization of high-frequency single crystal silicon (SCS) block resonators with piezoelectric electromechanical transducers. The resonators are fabricated on 4 μ m thick SOI substrates and use sputtered ZnO as the piezo material. The centrally-supported blocks can operate in their first and higher order length extensional bulk modes with high quality factor (Q). The highest measured frequency is currently at 210MHz with a Q of 4100 under vacuum, and the highest Q measured is 11,600 at 17MHz. The uncompensated temperature coefficient of frequency (TCF) was measured to be $-40\text{ppm}/^\circ\text{C}$ and linear over the temperature range of 20-100 $^\circ\text{C}$.

INTRODUCTION

With increasing demand for higher level of integration and lower cost in wireless and portable electronics, high- Q micromechanical resonators pose as choice candidates for integrated on-chip frequency references, filters, and sensors. Micromechanical resonators constitute a promising alternative to the existing resonator technology mainly due to their small size, ease of integration and superior performance. Therefore a rapidly growing interest has created a need to push the frequencies of micromechanical resonators into the ultra high frequency (UHF) band.

Several capacitively-transduced, silicon micromechanical resonators with high Q have been demonstrated [1-3]. However, extension of the operating frequency of capacitive MEMS resonators to the VHF and UHF range requires ultra-thin electrode-to-resonator gap spacing [1], introducing complexities in the fabrication process. Also in many applications, the series motional resistance R_m must be minimized for impedance matching purposes. This is usually done by increasing the dc bias voltage in capacitive resonators to $>10\text{V}$, which is often limited and not desirable.

In contrast to capacitive devices, the motional resistance in piezoelectric resonators is much smaller due to their higher electromechanical coupling. Examples of piezoelectric devices are surface and bulk acoustic wave resonators. The main drawback of surface acoustic wave (SAW) devices is their bulky size and incompatibility with silicon microelectronics. Film Bulk Acoustic Resonators (FBAR's) overcome the size issue and have GHz frequencies [4]. However, since FBAR's utilize the thickness longitudinal vibration of a piezoelectric film, accurate control of film

thickness across the wafer is critical for frequency stability and repeatability. In addition, multiple frequency devices/standards will need various piezo film thicknesses on a chip, complicating the manufacturing process.

In this paper, we report on silicon micromechanical resonators that operate in their in-plane length extensional bulk modes. Low-impedance electromechanical transducers are implemented by depositing very thin films of piezoelectric materials ($\sim 3000\text{\AA}$) such as zinc-oxide (ZnO) directly on the silicon resonator. The natural frequency of the resonators is to the first order independent of the film thickness and determined by resonator's lateral dimensions that are defined lithographically. Therefore, compared to the FBAR's, the resonators reported in this paper are much less sensitive to thickness variations in the thin films and have a simple three-mask low-temperature manufacturing process.

RESONATOR DESIGN

The first generation of the devices reported in this work were low-frequency clamped-clamped beam resonators ($f_{\text{resonant}} < 17\text{MHz}$) operating in their out-of-plane flexural modes [5]. The new class of resonators reported here extend the frequency of this technology into very high frequency (VHF range) by using in-plane length extensional bulk resonant modes, and alleviate the adverse effect of oxide undercut on the resonant frequency of the devices.

A. Mechanical Design

Fig. 1 shows a schematic diagram of the two-port block resonator described in this paper.

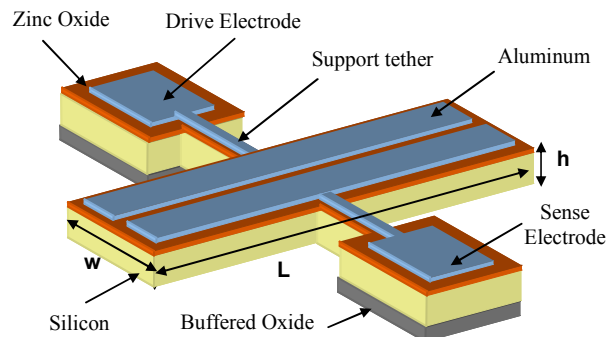


Fig. 1 Schematic of the piezo-on-silicon block resonator on SOI substrate with electrodes placed along the entire length of the block.

The structure of the resonator resembles that of a simple block, centrally supported by self-aligned small tethers. Single crystal silicon is used as the resonating element

because of its high inherent mechanical quality factor and stress free properties. Piezoelectric sense and actuation is provided by a thin ZnO film sputtered directly on silicon, sandwiched between the top aluminum electrodes and the bottom low resistivity SCS substrate. The ZnO film acts also as insulator between the top aluminum electrode and bottom device layer. The elimination of the bottom metal electrode conventionally used in piezoelectric devices is introduced to reduce the number of stacked layers, which could ultimately increase the quality factor of the resonator.

Stress is produced in the piezoelectric layer when a field is applied across the input electrode. Since the layers are structurally intact, normal forces are transferred from the piezoelectric film to the resonator body (device layer). In the vicinity of the resonance frequencies, the corresponding vibration mode will be excited, and the output is sensed from the net charge induced at the electrode on the opposite side of the resonator.

The shapes and natural frequencies of the length extensional modes of the block resonators are given by [6]:

$$u_n(x) = \cos \frac{n\pi x}{L} \quad \text{and} \quad \omega_n = \frac{n\pi}{L} \sqrt{\frac{E}{\rho_s}} \quad (1)$$

where n is the mode number ($n = 1, 2, 3, \dots$), L is the length of the block, and E and ρ are the Young's modulus and density of the structural material (Si), respectively. The inverse piezoelectric effect can only be detected when the electrodes possess a net charge. Hence, even modes cannot be detected and a response is observed only for odd-numbered modes.

B. Finite Element Analysis

Finite element modal analysis was performed in ANSYS to aid with the design of the block resonators. The block structure was originally intended to operate in the first and third length-extensional modes (Figs. 2 and 3). Since the zinc oxide and aluminum layers are relatively thin compared to the resonator body, the 3D model included only the anisotropic SCS block and support tethers. The support tethers are assumed to be perfectly clamped at the ends and are centrally located. The silicon block is tightly meshed with tetrahedral SOLID187 elements. Figs. 2 and 3 are contour plots of the displacement in the z direction (normal to the surface) overlaid on the mode shape. They show the first and third length-extensional modes for a $120\mu\text{m}$ long by $30\mu\text{m}$ wide centrally-supported silicon block at 35.7MHz and 104MHz, respectively.

C. Equivalent Electrical Model

Fig. 4 represents the equivalent LCR circuit model for the block resonator along with equations for its circuit elements. For full-length symmetrical electrodes, the electro-mechanical coupling coefficient is given by $\eta = 2d_{31}E_p b$, where b represents the width of the electrode. The capacitors C_{PAD} (drive and sense) model the static capacitance between the electrodes and the device layer. The two transformers in the model account for the isolation between the input and output electrodes.

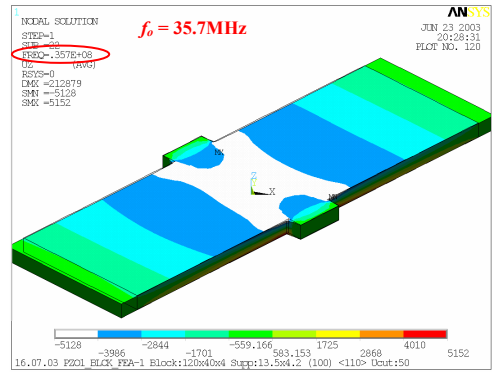


Fig. 2 ANSYS finite element modal analysis mode plot showing the 1st extensional mode in a $120\mu\text{m} \times 30\mu\text{m}$ block at 35.7MHz.

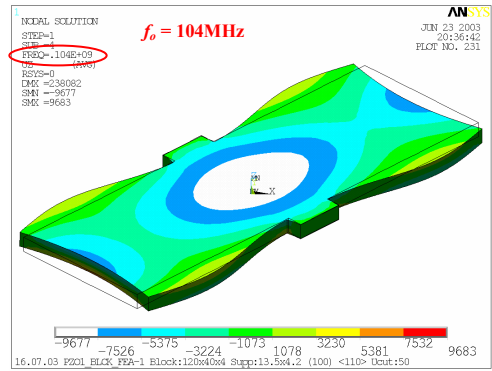


Fig. 3 ANSYS finite element modal analysis mode plot showing the 3rd extensional mode in a $120\mu\text{m} \times 30\mu\text{m}$ block at 104MHz.

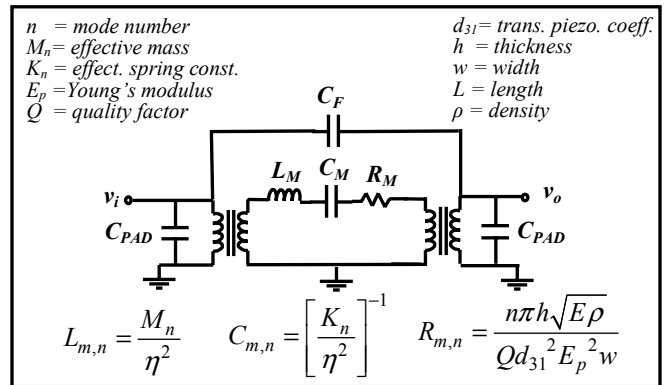


Fig. 4 Equivalent electrical model of the two-port block resonator.

RESONATOR FABRICATION

The fabrication process has three masks and is carried out on a silicon-on-insulator (SOI) substrate. Fig. 5 shows a brief fabrication process flow for the piezo-on-silicon block resonators. The resonator body is defined by etching shallow trenches ($4\mu\text{m}$ wide) into the device layer to land on the buffer oxide layer of the SOI substrate. The device layer of the selected SOI is (100) p-type low-resistivity with a nominal thickness of $4\mu\text{m}$. The length of the block is aligned along the $\langle 110 \rangle$ direction. The buffer oxide of SOI is wet etched in $\text{HF}/\text{H}_2\text{O}$ (1:1) to create a cavity underneath the resonating block.

The piezoelectric ZnO film is then sputtered on the silicon at a substrate temperature of 250°C, a pressure of 6mTorr, an Ar to O₂ mix ratio of 1:1, and an RF power of 300W [5]. The piezoelectric film has a thickness of 0.35μm and shows strong c-axis (002) orientation. The ZnO is then patterned by wet etching in NH₄Cl. Ammonium chloride (NH₄Cl) was chosen because of its slow etch rate (50Å/s) that enables definition of small ZnO features without severe lateral undercut. The Al top electrode (1000Å) is defined using the third mask in a lift-off process. Figures 6(a) and (b) show SEM pictures of two different dimensions of the fabricated block resonators.

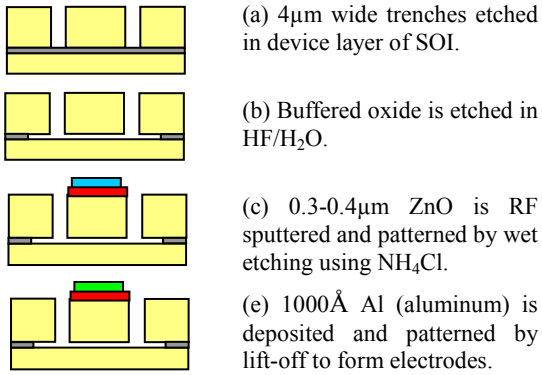


Fig. 5 Fabrication process flow for the piezo-on-silicon block resonator.

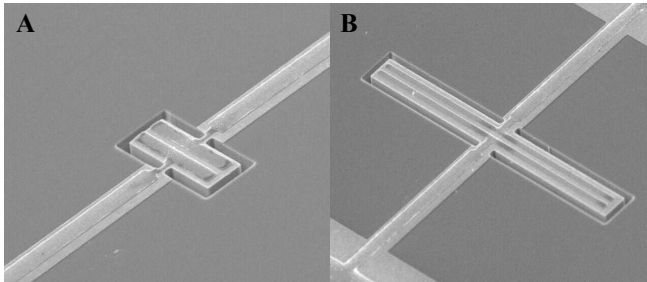


Fig. 6 SEM pictures of fabricated (a) 60μm×30μm and (b) 240μm×20μm piezo-on-silicon block resonators.

MEASUREMENT AND CHARACTERIZATION

The fabricated resonators were tested in a custom-built vacuum chamber at 50mTorr. Electrical contact to the resonator was made by wire bonding to the square shaped pads. Each pad has a parasitic capacitance of approximately 10pF to the device layer through the 0.35μm ZnO layer. The device layer was grounded to function as a bottom electrode. The resonator current was detected using a low noise amplifier and no attempt was made to impedance match the resonators to the interface circuitry. The frequency spectra of the resonators were captured using Agilent 4395A network analyzer. In contrast to the capacitive devices, piezoelectric resonators do not require a DC voltage to operate.

A. First and Third Order Extensional Modes

Fig. 7 shows the measured first and third length extensional modes for a 120μm×30μm piezo-on-silicon block resonator ($h=4\mu\text{m}$). The third mode is at 107MHz and has a Q of 4800 in vacuum. The measured resonant frequencies are in close

agreement with FEA results and analytical values found using (1). Similar modes were observed for blocks of varying dimensions and the results are summarized in Table 1. The highest frequency third order measured mode is currently at 210MHz with a Q of ~3,000 for a 60μm×30μm block. A quality factor of 11,600 for the first extensional mode of a 240μm×20μm at 16.9MHz is the highest Q recorded to date. An interesting fact to note is that the recorded Q values are higher for higher order modes in some of the tested devices.

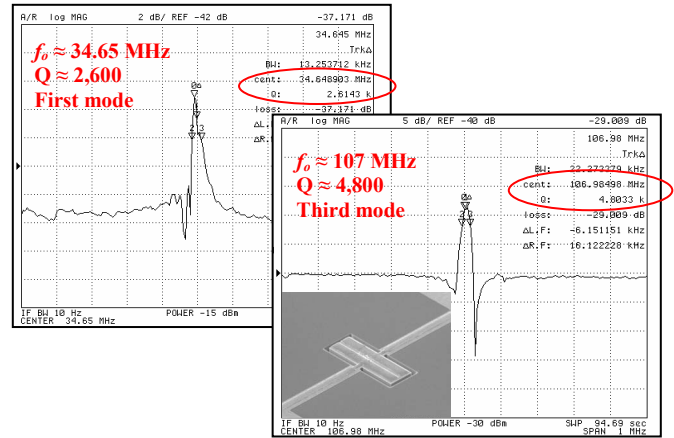


Fig. 7 First and third high- Q length extensional modes measured at 34.65MHz and 107MHz for a 120μm×30μm piezo-on-silicon block.

Table 1. Summary of quality factor and resonant frequency measurements in vacuum for fabricated piezo-on-silicon blocks of various lengths.

| Length × Width [μm] | Mode | Calculated f_0 [MHz] | Measured f_0 [MHz] | Measured Q |
|---------------------|------|------------------------|----------------------|--------------|
| 60×30 | 1 | 70 | 68 | 700 |
| | 3 | 212.4 | 210 | 2,984 |
| 120×30 | 1 | 35.4 | 35 | 2,600 |
| | 3 | 106.2 | 107 | 4,800 |
| 240×20 | 1 | 17.69 | 16.9 | 11,643 |
| 480×120 | 1 | 8.84 | 8.2 | 2,440 |
| | 7 | 61.9 | 67 | 5,500 |
| | n | - | 195 | 4,700 |
| 480×40 | n | - | 209.7 | 4143 |

Although capacitive silicon resonators have shown higher quality factors (~10X) at VHF frequencies [1, 3], the motional resistance of the piezo-on-silicon block resonators is much smaller than that of their capacitive counterparts. Using the equation given in Fig. 4, the motional resistances for the 1st and 3rd extensional modes of the 120μm×30μm piezo-on-silicon block resonator are calculated to be 9.5kΩ and 15.5kΩ, respectively (for $d_{31}=4.7\times 10^{-12}\text{coul/N}$, $E_p=123\text{GPa}$ [7]).

B. Higher Order Extensional Modes

Since the natural frequencies of the length extensional modes of the block structure grows with the mode number n , the use of higher order modes constitutes a key advantage in reaching high frequencies while keeping the structural dimensions in a range that can be easily fabricated. We

observed high- Q higher order modes for a $480\mu\text{m}\times 120\mu\text{m}$ block resonator. Fig. 8(a) shows a high order mode for this block at 66.7MHz with a Q of 5500, while Fig. 8(b) shows a higher order mode for the same device at 195.4MHz with a Q of 4700.

Figs. 9 and 10 show contour plots of the mode shapes found with ANSYS, confirming the peaks observed in Figs. 8(a) and 8(b), respectively. The repeating regions with identical strain fields prove these to be high order extensional modes.

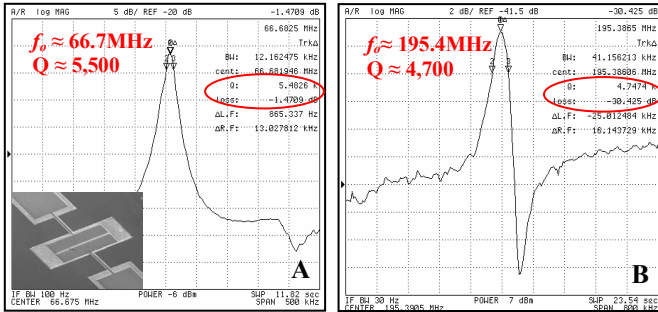


Fig. 8 Higher order extensional resonant modes measured at (a) 66.7MHz and (b) 195.4MHz, for a $480\mu\text{m}\times 120\mu\text{m}$ block resonator.

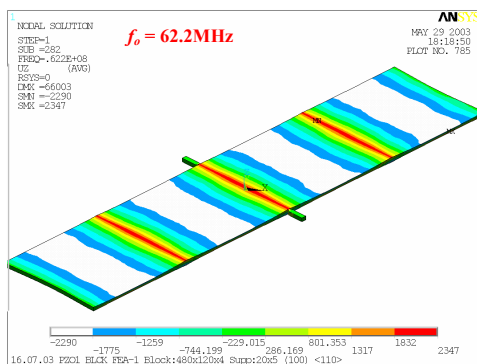


Fig. 9 ANSYS simulation showing higher order extensional mode in a $480\mu\text{m}\times 120\mu\text{m}$ block at 62.2MHz.

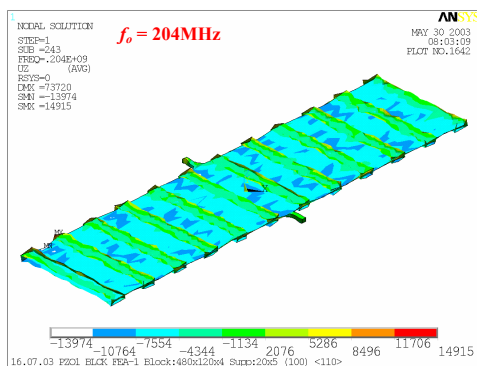


Fig. 10 ANSYS simulation showing higher order extensional mode in a $480\mu\text{m}\times 120\mu\text{m}$ block at 204MHz.

C. Temperature Coefficient of Frequency

Fig.11 shows the measured temperature characteristic of the $480\mu\text{m}\times 120\mu\text{m}$ block resonator operating at the 66.7MHz mode in the range of 20-100°C. The temperature coefficient of frequency (TCF) is linear and measured to be $-40\text{ppm}/^\circ\text{C}$. This is mainly caused by the temperature dependence of the

Young's modulus of single crystal silicon, reported to be $\approx -50\text{ppm}/^\circ\text{C}$ [8]. Solely from the temperature dependence of silicon, the expected TCF of these resonators should be $\approx -25\text{ppm}/^\circ\text{C}$. The stress relief of ZnO with temperature could further increase the TCF of these resonators.

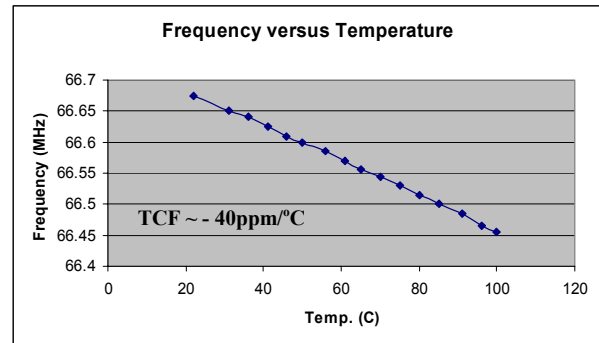


Fig. 11 Measured TCF for a $480\mu\text{m}\times 120\mu\text{m}$ block at 66.7MHz.

CONCLUSION

The design, fabrication and testing of high frequency piezo-on-silicon block resonators was reported in this paper. High mechanical quality factors ranging from 2,400 to 11,600 were demonstrated. The experimental results were confirmed with ANSYS finite element modal analyses. High order extensional modes were also actuated showing the ability to reach resonance frequencies as high as 210MHz.

ACKNOWLEDGEMENTS

This work was supported by DARPA under contract # DAAH01-01-1-R004. The authors wish to thank Dr. Zhili Hao and Pejman Monajemi for their contributions and the staff at Georgia Tech Microelectronics Research Center for their assistance.

REFERENCES

- [1] S. Pourkamali, F. Ayazi, "SOI-Based HF and VHF Single-Crystal Silicon Resonators with Sub-100 Nanometer Vertical Capacitive Gaps," *Digest of the 12th International Conference on Solid State Sensors, Actuators and Microsystems (Transducers'03)*, Boston, 2003, pp. 837-840.
- [2] S. Pourkamali, A. Hashimura, R. Abdolvand, G. K. Ho, A. Erbil, F. Ayazi, "High-Q single-crystal silicon HARPSS capacitive beam resonators with self-aligned sub-100-nm transduction gaps", *Journal of Microelectromechanical Systems*, vol. 12, N 4, August 2003, pp. 487-496.
- [3] J.R. Clark, W.-T. Hsu, C.T.-C. Nguyen, "High-Q VHF micromechanical contour-mode disk resonators", *IEEE Int. Electron Devices Meeting*, Dec., 2000, pp. 493-496.
- [4] R. Ruby, P. Bradley, J. Larson III, Y. Oshmyansky, D. Figueredo, "Ultra-Miniature High-Q filters and Duplexers using FBAR Technology", *ISSCC Digest of Technical Papers*, Feb. 2001, vol. 44, pp. 121-122.
- [5] G. Piazza, R. Abdolvand, F. Ayazi, "Voltage-tunable piezoelectrically-transduced single-crystal silicon micromechanical resonators on SOI wafer", *Proc. IEEE MEMS'03*, Kyoto, Japan, Jan. 2003, pp. 149-152.
- [6] S. S. Rao, *Mechanical Vibrations*, 3rd ed., Reading, MA: Addison-Wesley, 1995, pp. 512.
- [7] M. J. Madou, *Fundamentals of Microfabrication*, 2nd ed., Boca Raton, FL: CRC Press, 2002, pp. 560.
- [8] H. J. Mckim, "Measurement of elastic constants at low temperature by means of ultrasonic waves data for silicon and germanium single crystals and for fused silica", *Journal of Applied Physics*, vol. 24, 1953, pp. 988-997.